NASA TECHNICAL NOTE

NASA TN D-5602

c. 1

NASA TN D-5602

INVESTIGATION OF LEVEL-FLIGHT AND MANEUVERING CHARACTERISTICS OF A HINGELESS-ROTOR COMPOUND HELICOPTER

by Julian L. Jenkins, Jr., and Perry L. Deal

Langley Research Center
Langley Station, Hampton, Va.

NATIONAL AERONAUTICS AND SPACE ADMINISTRATION • WASHINGTON, D. C. • JANUARY 1970

1. Report No. NASA TN D-5602	2. Government Accession No.	3. Recipient's Catalog No.
4. Title and Subtitle INVESTIGATION OF LEVEL-FLIGHT AND MANEUVERING CHARACTERISTICS OF A HINGELESS-ROTOR COMPOUND HELICOPTER		5. Report Date January 1970 6. Performing Organization Code
7. Author(s) Julian L. Jenkins, Jr., and Perry L. Deal		8. Performing Organization Report No. L-6661 10. Work Unit No. 721-05-10-06-23
9. Performing Organization Name and Address NASA Langley Research Center Hampton, Va. 23365		11. Contract or Grant No. 13. Type of Report and Period Covered Technical Note
12. Sponsoring Agency Name and Address National Aeronautics and Space Administration Washington, D.C. 20546		14. Sponsoring Agency Code

15. Supplementary Notes

16. Abstract

The results of a flight-test program utilizing a hingeless-rotor compound helicopter are presented and discussed. Data are presented to indicate the level-flight performance characteristics, speed stability, maneuver stability, and wing-rotor lift sharing in maneuvering flight. Also included are data indicating the rotor rotational-speed control characteristics during maneuvers and during simulated main-rotor power failures.

The data show that there is an inherent reduction in rotor lift as level-flight airspeed is increased. In addition, a reduction in rotor-lift sensitivity in maneuvering flight was measured and determined to be dependent on the stability of the aircraft in maneuvering flight. Although the lift-sharing trends contribute favorably to the piloting task in the compound mode, the rotor overspeed tendencies could require constant pilot attention during maneuvering flight.

17. Key Words Suggested by Author(s)	18. Distribution Statement
Rotary wing Compound helicopter Hingeless rotor	Unclassified – Unlimited

19. Security Classif. (of this report)	20. Security Classif. (of this page)	21. No. of Pages	22. Price*
Unclassified	Unclassified	31	$3.00

*For sale by the Clearinghouse for Federal Scientific and Technical Information Springfield, Virginia 22151

INVESTIGATION OF LEVEL-FLIGHT AND MANEUVERING CHARACTERISTICS OF A HINGELESS-ROTOR COMPOUND HELICOPTER

By Julian L. Jenkins, Jr., and Perry L. Deal
Langley Research Center

SUMMARY

The results of a flight-test program utilizing a hingeless-rotor compound helicopter are presented and discussed. Data are presented to indicate the level-flight performance characteristics, speed stability, maneuver stability, and wing-rotor lift sharing in maneuvering flight. Also included are data indicating the rotor rotational-speed control characteristics during maneuvers and during simulated main-rotor power failures.

The data show that there is an inherent reduction in rotor lift as level-flight airspeed is increased. In addition, a reduction in rotor-lift sensitivity in maneuvering flight was measured and determined to be dependent on the stability of the aircraft in maneuvering flight. Although the lift-sharing trends contribute favorably to the piloting task in the compound mode, the rotor overspeed tendencies could require constant pilot attention during maneuvering flight.

INTRODUCTION

The desirability of increasing the high-speed performance and maneuvering ability of rotary-wing aircraft has been recognized for some time. Theoretical and experimental studies have demonstrated the problems associated with rotor operation at high speed. (See refs. 1 and 2.) These studies indicate a decrease in the lifting and propulsive capability of the rotor as speed increases. Consequently, in order to maintain the hovering and low-speed capabilities of a rotor while improving high-speed performance, additional sources of lift and/or propulsive force are required.

In recent years, several helicopters have been modified to incorporate various methods of compounding (i.e., the addition of auxiliary propulsion and/or wings) in order to verify the expected improvements in high-speed performance and to define the problems associated with high-speed rotary-wing aircraft. These test-bed compound aircraft were modified and tested under contracts by the U.S. Army.

This report presents flight-test results obtained during a program by the National Aeronautics and Space Administration utilizing a hingeless-rotor compound helicopter. Program support was provided by the U.S. Army. Data are presented to indicate the level-flight performance characteristics, speed stability, maneuver stability, and wing-rotor lift sharing in maneuvering flight. Also included are data indicating the rotor rotational-speed control characteristics during maneuvers and during simulated main-rotor power failures.

SYMBOLS

B_1 longitudinal control position, positive in nose-down direction, degrees

b number of blades

C_{L_R} rotor lift coefficient, $\frac{L_R}{\rho\pi R^2(\Omega R)^2}$

$C_{L_{wb}}$ wing-body lift coefficient, $\frac{L_{wb}}{q_\infty S_w}$

$\left(C_{L_\alpha}\right)_{wb}$ lift-curve slope for wing-body, $\frac{\partial C_{L_{wb}}}{\partial \alpha_B}$

c blade chord, feet (meters)

F_N auxiliary jet thrust, pounds force (newtons)

F_{δ_y} longitudinal cyclic-stick force, pounds force (newtons)

g acceleration due to gravity, 32.2 ft/sec^2 (9.8 m/sec^2)

L_R rotor lift, pounds force (newtons)

L_{wb} wing-body lift, pounds force (newtons)

n aircraft vertical load factor, $\frac{L_R + L_{wb}}{W}$

P_e equivalent total horsepower, $P_i + \frac{F_N V_{TAS}}{326}$, horsepower (kilowatts)

P_i indicated shaft horsepower, horsepower (kilowatts)

p	aircraft roll rate, positive with right roll, degrees/second
q	aircraft pitch rate, positive nose-up, degrees/second
q_∞	free-stream dynamic pressure, pounds force/foot^2 (newtons/meter^2)
R	rotor radius, feet (meters)
S_W	wing area, feet^2 (meters^2)
V_{CAS}	calibrated airspeed, knots
V_{TAS}	true airspeed, knots
W	aircraft gross weight, pounds force (newtons)
α_B	boom-indicated angle of attack, angle of fuselage reference line relative to wind, positive nose-up, degrees
α_C	rotor control-axis angle of attack, positive when tilted rearward, degrees or radians as indicated
β	aircraft sideslip angle, positive nose left, degrees
δ_x	lateral stick position, positive for right deflection, inches (centimeters)
δ_y	longitudinal stick position, positive for rearward deflection, inches (centimeters)
θ	blade-root pitch angle, degrees
θ_0	blade-root collective-pitch angle, degrees
ρ	air density, slugs/foot^3 (kilograms/meter^3)
σ	rotor solidity, $\frac{bc}{\pi R}$
Ω	rotor angular velocity, radians/second

APPARATUS AND TESTS

Description of Test Aircraft

The test aircraft, shown in figure 1, was a compound helicopter which incorporates a hingeless-rotor system. The aircraft is described in more detail in reference 3. The basic physical characteristics of the test aircraft are presented in table I.

The flight-control systems are basic helicopter-type controls, and there are no movable fixed-wing-type control surfaces incorporated. The aircraft is equipped with the standard XH-51A mechanical control gyro. The auxiliary power system required an additional control which is incorporated in the twist grip of the collective-pitch handle. Because of this modification, the primary power control is installed on a quadrant mounted to the left of the collective-pitch lever.

The cyclic-stick control has an irreversible boost with a longitudinal feel spring (8 lbf/in. (14 N/cm)). A bobweight (7.2 lbf/g unit (32 N/g unit)) was also incorporated into the longitudinal control. Total stick travels were 10 inches (25.4 cm) and 4.625 inches (11.7 cm) for the longitudinal and lateral directions, respectively.

For the test results presented herein, the longitudinal cyclic control was set at 66 percent of the designed stick gearing, and the lateral cyclic control was set at 200 percent of the designed stick gearing. These changes simply alter the pilot's cyclic-stick displacement required to produce a given aircraft response rate. The change in the longitudinal system, for example, reduces the response rate for a given stick displacement to 66 percent of the rate which would be achieved with the standard stick gearing.

Instrumentation

The instrumentation utilized during these tests was installed and calibrated by the contractor. Data were recorded on a 50-channel oscillograph and a photo recorder.

Tests

The flight-test program consisted of approximately 9 hours of operation including the pilot's familiarization flights. The tests were accomplished in two phases. Since these tests were not intended to extend the operating envelope of the aircraft, the data obtained were limited to airspeeds up to approximately 190 knots calibrated airspeed and a specified range of rotor loading (i.e., collective-pitch angles).

The flight conditions investigated included level flight throughout the allowed forward-speed range, autorotation entries, maneuver characteristics, cyclic-control response characteristics, and rotor rotational-speed control in maneuvers.

RESULTS AND DISCUSSION

The data presented herein include the level-flight performance characteristics, speed stability, and maneuver stability for several airspeeds and also data indicating the lift-sharing characteristics during maneuvering flight. Also included are data indicating the rotor rotational-speed control characteristics during maneuvers and during simulated main-rotor power failures.

The majority of the test points were taken with a nominal collective-pitch setting of 3.5°. This value represents the recommended pitch setting for compound-mode flight (i.e., airspeeds above approximately 100 knots). Thus, once the airspeed exceeded 100 knots, the collective pitch could be set to the desired position of 3.5°, and the aircraft could be flown essentially as a fixed-wing aircraft with speed variations being made by throttle control of the auxiliary thrust engine.

Level-Flight Performance

The primary level-flight performance characteristics of the test vehicle are presented in figures 2 to 6. These data were obtained at a density altitude of approximately 5700 feet (1.7 km).

Rotor lift and indicated angle of attack.- The variation of the ratio of rotor lift to gross weight with true airspeed for a range of collective-pitch settings is presented in figure 2. For the recommended compound-mode setting of 3.5°, the rotor lift is equivalent to 57 percent of the gross weight at 110 knots and decreases almost linearly with increasing airspeed. Extrapolation indicates that the rotor would be completely unloaded at approximately 240 knots. Increasing collective pitch, of course, increases the relative rotor loading; however, the maximum airspeed at the higher collective-pitch setting is restricted by an early onset of vibrational problems. Thus, a collective-pitch setting in the range from approximately 3.5° to 4.3° provides the maximum range of airspeed wherein the aircraft can be flown without need for a collective-pitch change. In addition to minimizing the pilot workload, by maintaining constant collective pitch, the trend of decreasing rotor lift as airspeed increases is advantageous. As the rotor penetrates a more unfavorable environment at the higher speeds, the gradual unloading of rotor lift tends to eliminate problems associated with rotor stall.

There are limitations at both ends of the airspeed range. First, as indicated in figure 2, the rotor may be completely unloaded at about 240 knots and would probably produce negative lift above this airspeed, with obvious performance penalties. Second, with the low collective-pitch setting, the aircraft angle of attack increases rapidly as the airspeed is reduced toward 100 knots. For example, the variation of the level-flight fuselage angle of attack with true airspeed is presented in figure 3. The lower

collective-pitch setting requires an excessive nose-high angle of attack in order to achieve the required lift on both the wing and rotor. Thus, flight at airspeeds near 100 knots can be accomplished more comfortably by employing a higher collective-pitch setting.

Thrust and power requirements.- The auxiliary thrust and power requirements for the test aircraft are presented in figures 4 to 6. Figure 4 presents the auxiliary thrust requirements for a range of collective-pitch settings. The thrust levels are indicated in terms of an equivalent flat-plate drag area because this parameter reflects the nose-high attitude requirements for the low collective-pitch settings at the lower speeds. In addition, the rotor attitude is such that a drag force is produced instead of a propulsive force since the rotor is very close to an autorotative condition at the low collective-pitch setting. As illustrated in figure 5, the rotor power requirements decrease with decreasing collective pitch; however, the auxiliary jet thrust must be increased to compensate for this decrement. In order to ascertain the total power requirements of the aircraft, an equivalent total horsepower which includes both the rotor-shaft horsepower and the jet thrust has been computed and is presented in figure 6. The data in this figure encompass all the collective-pitch settings utilized. Within the scatter of the data, it would appear that the total power requirements at a given airspeed are the same regardless of the collective pitch selected.

Wing-body lift coefficient.- The wing-body lift coefficient is presented in figure 7 as a function of the boom-indicated fuselage angle of attack for the range of test airspeeds. These data were obtained in level flight and have been corrected for the jet-reaction effect due to inclination of the jet thrust axis. By using a least-squares curve fit, a lift-curve slope of 0.0606 per degree (3.47 per radian) is indicated.

Control Response

The longitudinal and lateral cyclic-stick response characteristics were evaluated for a range of airspeeds. The results are presented in figure 8 as a function of the aircraft pitch or roll rate per inch (centimeter) of stick deflection. It should be recalled that these tests were performed with the stick gearing set at off-design conditions and that the rotor has a mechanical control gyro which has a significant effect on the response. The data include the response characteristics at several collective-pitch settings although no significant effect on response is apparent for most of the settings. At the highest collective-pitch setting $(\theta_0 = 6^\circ)$ where there is a relatively large change in rotor lift, the response about both axes appears to be slightly higher as might be expected; however, since the rotor hub moment is the more significant part of the total rotor moment, the gradient with increasing airspeed is primarily dependent on the increased hub-moment sensitivity. Although the magnitude and gradient with airspeed of the longitudinal

response sensitivity are low, some difficulty would be expected in achieving compatible response characteristics at both low and high speeds. Limited hover and low-speed qualitative evaluation indicated that the longitudinal response was less than desired.

Stability Characteristics

Speed stability.- The speed stability of the test aircraft was evaluated for several trim airspeeds. These data, which are presented in figure 9, were obtained by establishing a trimmed level-flight condition at a given airspeed and making slow variations in airspeed about the trim point. As indicated, the longitudinal stick position δ_y has a slightly unstable slope for all test airspeeds. The slope of the stick position is also slightly unstable about the trim point for increased rotor loading at 109 knots $(\theta_0 = 6.8^o)$.

Although the data are indicative of an instability with speed, the gradient is so small that the pilot's impression was that the aircraft had neutral stability. In view of the fact that these data were obtained at reduced longitudinal stick sensitivity which necessitates larger stick deflections, the gradient of stick position with speed would be reduced as stick sensitivity is increased.

Maneuver stability.- Two techniques were utilized to evaluate the maneuver stability of the test aircraft. The first technique employed was the windup turn to obtain the stick force per g unit, and the second technique was the pull-and-hold maneuver normally utilized for pure helicopters.

The results of the windup turn maneuvers are presented in figure 10 as the variation of the measured longitudinal stick force per unit load factor over the range of test airspeeds. Also included are the variations in stick sensitivity (g units per inch (centimeter) of stick deflection) and the angle-of-attack sensitivity (g units per radian change in fuselage angle of attack).

In all cases, the aircraft exhibited positive maneuver stability (that is, a positive stick displacement and force gradient); however, the pilot felt that the force gradient was high at the lower speeds. Since the force gradient results from an artificial feel system which is dependent on stick displacement and load factor, some latitude in providing a suitable gradient was available. The stick force gradient can also be determined with the following expression:

$$\left.\begin{aligned} \frac{dF_{\delta_y}}{dn} &= \frac{8.0}{dn/d\delta_y} + 7.2 \qquad \text{lbf/g unit} \\ \frac{dF_{\delta_y}}{dn} &= \frac{35.6}{dn/d\delta_y} + 32.0 \qquad \text{N/g unit} \end{aligned}\right\} \tag{1}$$

The parameter $dn/d\delta_y$ is presented in figure 10 for a control gearing of 66 percent of the designed gearing. Thus, increasing the control gearing or decreasing the feel-spring constant would produce a lower stick force gradient. At the higher speeds, the pilot felt that the combination of stick force gradient and stick sensitivity were at a satisfactory level. It should be pointed out, however, that no attempt was made to evaluate other combinations of artificial force gradient.

The last parameter $dn/d\alpha_B$ presented in figure 10 is a measure of the overall aircraft sensitivity in maneuvers. As a result of the influence of the rotor it will be noted that the sensitivity $dn/d\alpha_B$ increases at a rate considerably less than the velocity squared of a fixed-wing aircraft. The dashed-line curve indicates calculated values based on the rotor lift derivatives given in reference 4 and the measured lift-curve slope of the wing-body combination. For this calculation, it was assumed that no change in rotor cyclic pitch was introduced; hence, the calculated curve is a measure of the effective controls-fixed sensitivity of the aircraft. The measured data, of course, include the effect of the rotor control variations required to perform the maneuvers. The equation used for the calculation is as follows:

$$\frac{dn}{d\alpha_B} = \frac{\partial\left(C_{L_R}/\sigma\right)}{\partial\alpha_C}\left(1 - \frac{dB_1}{d\alpha_B}\right)\frac{\sigma\rho\pi R^2(\Omega R)^2}{W} + \frac{\partial C_{L_{wb}}}{\partial\alpha_B}\frac{q_\infty S_W}{W} \tag{2}$$

where $dB_1/d\alpha_B$ is assumed to be zero.

The measured sensitivity appears to be higher than the controls-fixed calculation at airspeeds below 155 knots and is lower than the calculation above 155 knots. As will be illustrated subsequently, these results are compatible since the measured values of $dB_1/d\alpha_B$ are negative at the lower speeds and positive at the higher speeds. Therefore, as noted in equation (2), a negative value of $dB_1/d\alpha_B$ will increase the total aircraft sensitivity $dn/d\alpha_B$; whereas, a positive value will decrease the calculated sensitivity.

The reversal in sign of the term $dB_1/d\alpha_B$ is indicative of a change in the level of angle-of-attack stability of the aircraft. When $dB_1/d\alpha_B$ is negative, the aircraft is stable; whereas, a positive value indicates an unstable system. Even though the stick-position gradient is positive (fig. 10) throughout the test airspeed range, the actual control position, as commanded by the mechanical control gyro on this aircraft, reverses direction in order to provide positive angle-of-attack stability at the higher speeds.

The reversal of control position is quite evident in the pull-and-hold maneuver illustrated in figure 11. For the condition presented, the aircraft response to a 1-inch-rearward (2.54 cm) cyclic input is indicative of a stable system. That is, both the rate and normal acceleration are concave downward in less than 2 seconds, and the stick displacement (and, consequently, the stick force) remains rearward. (See ref. 5.) The

blade pitch angle, however, is indicative of a different trend. The cyclic amplitude is approximately 2° (i.e., $B_1 = 2^{\circ}$) nose-down in level flight, which is consistent with the forward stick position. After the longitudinal stick position is displaced rearward, the blade cyclic-pitch amplitude decreases as expected; and then with constant stick position, the amplitude increases beyond the original trim (i.e., $B_1 > 2^{\circ}$). The reversal in blade cyclic pitch relative to that commanded by the stick position is introduced by the mechanical control gyro in providing apparent maneuver stability to the pilot. This reversal in blade cyclic pitch during maneuvers also has a favorable effect on the rotor loading.

Wing-Rotor Load Sharing in Maneuvers

Measured rotor-lift sensitivity.- Of particular importance with regard to flight in the compound mode is the relative load sharing between the wing and the rotor during maneuvers. Windup turns were executed in order to establish the rotor-lift variation with load factor for several airspeeds. The results are presented in figure 12. The data presented were taken at a nominal collective-pitch setting of 3.5°. The variation in rotor lift at 1.0g merely reflects the level-flight lift variation previously indicated (fig. 2). The data indicate that the rotor is providing a smaller increment of lift for a given load factor at the higher airspeeds.

In order to illustrate this trend more clearly, the rate of change of the rotor loading with load factor $\frac{d(L_R/W)}{dn}$ was determined and is plotted as a function of airspeed in figure 13. Since the rotor loading with load factor was essentially independent of collective pitch, figure 13 includes data applicable to all tested collective-pitch values. The curve illustrates the effective decrease in the rotor-lift sensitivity with increasing airspeed. For example, in the turning maneuver the rotor provides approximately 73 percent of the incremental lift at 120 knots, but only 44 percent of the incremental lift at 210 knots. The reduction in lift sensitivity with speed is very beneficial since the rotor produces lower lift increments during maneuvers as it penetrates the more unfavorable environment at higher speeds.

Calculated rotor sensitivity (controls fixed).- In order to illustrate the unusual rotor-loading trend of the test aircraft, a calculated curve based on the theoretical rotor lift derivative is included in figure 13. The equation used is as follows:

$$\frac{d(L_R/W)}{dn} = \frac{\rho \pi R^2 (\Omega R)^2 \sigma}{W} \frac{\partial (C_{L_R}/\sigma)}{\partial \alpha_C} \frac{d\alpha_C}{dn} \tag{3}$$

where $d\alpha_C/dn$ is assumed to be equal to the inverse of the measured parameter $dn/d\alpha_B$ (fig. 10). Thus the calculation represents the expected rotor-lift sensitivity with blade cyclic controls fixed. The difference in trends is obvious. The measured

curve, of course, was obtained with cyclic-control inputs, and thus the change in rotor angle of attack with load factor would differ from the fuselage angle of attack α_B used.

Calculated rotor sensitivity (including control displacement).- The actual change in rotor angle of attack with load factor may be expressed as follows:

$$\frac{d\alpha_C}{dn} = \frac{d\alpha_B}{dn} - \frac{dB_1}{dn} \tag{4}$$

It should be noted that stable maneuver stability requires a negative sign for dB_1/dn. The negative sign, however, makes the parameter $d\alpha_C/dn$ larger than $d\alpha_B/dn$ and would increase the rotor-loading sensitivity. Unstable maneuver stability, on the other hand, requires a positive sign for dB_1/dn, thus decreasing the rotor-loading sensitivity. It would appear from figure 13, therefore, that above approximately 150 knots the aircraft has negative angle-of-attack stability.

Although it was indicated in figure 10 that the aircraft had positive maneuver stability as apparent to the pilot (stick position and force) over the test airspeed range, an analysis of these data indicates that there is considerable cyclic-pitch feedback occurring during maneuvers which is produced by the mechanical control gyro. For example, figure 14 illustrates the measured variation of the longitudinal cyclic-pitch increment (ΔB_1) with load factor for several airspeeds. The increment ΔB_1 is the difference between the longitudinal cyclic pitch in level flight and the value in the turn. It is actually a combination of the pilot input and the control-gyro feedback. It should be recalled (fig. 10) that in all cases a rearward stick displacement was required to maintain a given load factor; however, the steady-state longitudinal cyclic pitch is shown to be in the opposite direction at the airspeeds above approximately 150 knots. In other words, the feedback required at higher speeds is large enough to wash out the pilot's rearward cyclic input (i.e., a negative B_1 increment) and actually produce a positive cyclic-pitch increment. Thus, as speed increases, the effective rotor angle-of-attack change in maneuvers becomes progressively smaller. This characteristic, in turn, reduces the rotor-lift sensitivity in maneuvers as airspeed is increased.

As an illustration of the effect on the lift sensitivity of including the actual rotor cyclic control, the calculated curve presented in figure 13 has been recomputed to include the cyclic terms shown in figure 14. The corrected points are presented in figure 15. The improvement in correlation is apparent. Although the 210-knot data point is somewhat high, the overall trend of sensitivity is well defined.

An alternate method for predicting load sharing is to use the lift-curve slope for the wing-body. The curve in figure 15 labeled "calculated using $(C_{L_\alpha})_{wb}$" was computed with the following equation:

$$\frac{d(L_R/W)}{dn} = 1 - \left(C_{L_\alpha}\right)_{wb} \frac{q_\infty S_W}{W} \frac{d\alpha_B}{dn} \tag{5}$$

where $\left(C_{L_\alpha}\right)_{wb} = 3.47$ per radian. (See fig. 7.)

The parameter $d\alpha_B/dn$ is the measured value obtained from figure 10 (the inverse of $dn/d\alpha_B$). It should be noted that the lift-curve slope used was obtained from level-flight data and therefore does not reflect the effects of pitch rate. Pitch rate would be expected to increase the effective wing-body loading contribution due to the horizontal tail and thus improve the correlation between the two curves. Nevertheless, the trend of the measured rotor loading is well defined.

Although the trend of decreasing rotor-lift sensitivity with increasing airspeed is advantageous with regard to avoidance of rotor-stall problems, it should be emphasized that the decreasing sensitivity occurs as a result of decreasing aircraft stability and an unstable rotor-fuselage configuration at the higher speeds. In this particular aircraft, however, the control gyro provides the stabilizing inputs required without pilot action. Thus, even though the pilot's cues (i.e., stick position and force) are indicative of apparent stability, the actual control position is not. Without the gyro, the maneuvering characteristics would, of course, be the same except that the pilot would have to provide the stabilizing inputs by moving the stick forward. In either case, the favorable rotor-loading trends result in reduced forward-control capability and, with the gyro in the system, the pilot is unaware of the remaining control margins. Although not encountered during the program, there may be combinations of airspeed and load factor that would utilize the maximum available nose-down cyclic pitch. Once this condition is reached, the aircraft would be divergent with a further increase in the angle of attack.

Rotor Rotational-Speed Control

Rotor rotational-speed control is important with regard to both the power-off autorotational characteristics and the maneuver overspeed characteristics. Since both of these characteristics are related to the load factor required to autorotate the rotor in a banked turn, criteria which define these load factors are adequate for establishing the maneuver overspeed trends as well as the power-off autorotational requirements. Tests were accomplished to establish the rotor rotational-speed (rpm) variation with load factor for the aircraft. The procedure was to establish a trim level-flight condition for the desired configuration and then to reduce main-rotor power to flight idle while entering a descending banked turn at constant airspeed and jet thrust. The rotor speed was allowed to drop to 90 percent of the design rpm. When a steady load factor for maintaining 90 percent rpm was established, the load factor was gradually increased in order to increase the rotor rpm.

Samples of the resulting data are presented in figure 16 for two airspeeds. The boundary lines indicate the combinations of rpm and aircraft load factor that will produce autorotation: that is, the shaft power is zero. The area to the left of each boundary represents the envelope wherein shaft power must be supplied to drive the rotor. Conversely, to the right of the boundary, the rotor extracts energy over and above that required to autorotate and would speed up in order to reestablish equilibrium on the autorotation boundary.

From the standpoint of maintaining rotor rpm in the event of a main-rotor power failure, the boundary represents the load factor necessary to prevent an underspeed condition, assuming no other corrective action is taken. For example, at 115 knots calibrated airspeed, the rotor would stabilize at 100 percent rpm if a load factor of approximately 1.3g was maintained. At 160 knots, the load factor for 100 percent rpm has increased to 1.8g.

In terms of rotor overspeed, the same data may be interpreted as a maneuver restriction in powered flight. If at a constant airspeed the load factor is increased beyond that required to autorotate the rotor, the rpm will increase from the initial setting. Figure 17 illustrates typical variations of power-on rpm with load factor for two different initial rotor speeds at 115 knots calibrated airspeed. The initial rise in rotor rpm as load factor increases is a function of the power governing loop. As the power demand is decreased, the governor reduces the supplied power and, therefore, the rpm remains essentially constant. However, as the load factor increases further, the shaft power required reaches zero (on the autorotation boundary) and the rpm rises along the boundary line as indicated. For the case illustrated, a steady load factor of 1.6g would produce a final rotor rpm in excess of 110 percent regardless of the initial governed rpm.

In order to illustrate the effectiveness of changes in aircraft configuration, a summary plot is presented in figure 18. Included in the figure are the effect of increasing the collective-pitch setting to a value above the normal compound mode of 3.5° and the effect of deploying the wing spoilers at the normal collective position. The boundary lines indicate the load-factor requirements to maintain a specified rpm as a function of the airspeed. The upper boundary (110 percent) can be associated with the power-on maneuver overspeed since any combination of airspeed and load factor which is above the boundary would drive the rotor rpm to values greater than 110 percent. For example, the data in figure 18(b) indicate that for a 2g maneuver the rotor speed would exceed 110 percent for airspeeds up to approximately 150 knots calibrated airspeed. The lower boundary, on the other hand, is an indication of the load factor which must be achieved in order to stabilize the power-off rotor rpm at 90 percent.

Changes in configuration can be accomplished in order to shift the boundaries in the desired direction. For example, figure 18(a) shows the effect of an increase in

collective pitch which effectively increases the maneuver overspeed boundary. Figure 18(c) shows the effect of application of wing spoilers as a means of lowering the boundary for the power-off autorotation. These changes in configuration indicate that the boundaries can be shifted with appropriate pilot action; however, this requires the pilot to monitor rotor rpm in order to prevent rotor overspeeds in maneuvers.

Autorotational Characteristics

Rotor rotational-speed decay rate.- Tests were performed to establish the rotor rpm decay rate following a loss of the primary power supply. The data, which were obtained at fixed collective pitch for several airspeeds, are presented in figure 19. The relatively low decay rates established result primarily from the low horsepower requirements of the rotor over the test airspeed range. (See fig. 5.) As might be expected, the trends of the decay rates reflect the changes in horsepower requirements shown in figure 5. Consequently, as the power required increases at the higher forward speeds, the rotor rpm decay rate also rises. The decay rates, however, are lower than those generally demonstrated by a pure helicopter which, of course, operates with higher rotor power requirements. The benefits associated with the low decay rates are offset at the higher airspeeds by the increase in the load-factor requirements for autorotating the rotor. (See, for example, fig. 18.) The rising decay rate and increasing load-factor requirements necessitate prompt action by the pilot in order to make an autorotative entry at the higher speeds.

Autorotative entries.- Autorotative entries following a simulated main-rotor power failure were made for a range of trim airspeeds from approximately 110 to 215 knots true airspeed. The same general maneuver was used to arrest the rotor rpm decay. That is, the pilot initiated a windup turn in order to place the rotor into an autorotative condition. In addition to performing this maneuver, the pilot had recourse to additional actions in order to arrest the rotor rpm decay. These included application of wing lift spoilers, reduction of auxiliary thrust, and a reduction of rotor collective pitch if necessary.

A sample autorotative entry is presented in figure 20. The simulated main-rotor power failure was initiated at a calibrated airspeed of 174 knots. The rotor speed was allowed to decay to 95 percent prior to taking any corrective action. For this entry, the pilot made an abrupt auxiliary-thrust reduction at 3.6 seconds (2.6 seconds after main-rotor power reduction) and deployed the spoilers at 5 seconds. Both of these actions produce a nose-down trim change, and the pilot reported that the trim shift was somewhat distressing with this sequence of abrupt action. All other entries were performed by using a more gradual reduction in auxiliary thrust; however, this abrupt maneuver serves

to emphasize the necessity of minimizing the trim shifts associated with corrective actions in an autorotative entry.

Throughout the airspeed range of the test, the rotor speed could be allowed to drop to 95 percent, and then with corrective action the rpm was maintained above 90 percent. The allowable delay time was, of course, decreasing as indicated by the rising decay rates in figure 19. Thus, at the higher speed relatively prompt action would be required.

CONCLUDING REMARKS

The flight-test results presented and discussed herein have indicated several trends which are of interest concerning both the performance and the flying qualities of compound helicopters. Specifically, the inherent reduction in rotor lift as level-flight airspeed is increased is desirable since no pilot action is required, and the reduced trim lift provides a margin between trim lift and the lifting capability of the rotor which may be utilized in maneuvers.

The trend of decreasing rotor-lift sensitivity in maneuvers with increasing airspeed is also advantageous with regard to avoidance of rotor-stall problems; however, it should be emphasized that in this case the decreasing sensitivity occurs as a result of decreasing aircraft stability and an unstable rotor-fuselage configuration at the higher speeds.

Although these lift-sharing trends contributed favorably to the piloting task in the compound mode, the rotor overspeed tendencies could require constant pilot attention during maneuvering flight.

High-speed autorotative entries could be made without undue pilot effort as a result of the low power requirements of the rotor which produced relatively low rotor rotational-speed decay rates. Adverse trim changes associated with any corrective actions should be minimized so that positive pilot response does not introduce undesirable disturbances.

Langley Research Center,
National Aeronautics and Space Administration,
Langley Station, Hampton, Va., October 27, 1969.

REFERENCES

1. Robinson, Donald W., Jr.: Use of Thrust and Lift Augmentation for Increasing Helicopter Operating Speed. Pap. No. 63-94, Inst. Aerosp. Sci., Jan. 1963.

2. Van Wyckhouse, J. F.; and Cresap, W. L.: High-Performance Helicopter Program. Summary Report, Phase II. TRECOM Tech. Rep. 64-61, U.S. Army, Oct. 1964.

3. Wyrick, Donald R.: Extension of the High-Speed Flight Envelope of the XH-51A Compound Helicopter. USAAVLABS Tech. Rep. 65-71, U.S. Army, Nov. 1965. (Available from DDC as AD 627 372.)

4. Kisielowski, E.; Perlmutter, A. A.; and Tang, J.: Stability and Control Handbook for Helicopters. USAAVLABS Tech. Rep. 67-63, U.S. Army, Aug. 1967. (Available from DDC as AD 662 259.)

5. Anon.: Helicopter Flying and Ground Handling Qualities; General Requirements for. Mil. Specif. MIL-H-8501A, Sept. 7, 1961, Amendment I, Apr. 3, 1962.

TABLE I.- PHYSICAL CHARACTERISTICS OF TEST AIRCRAFT

General:	
Nominal take-off weight, lbf (N)	5165 (22 974)
Longitudinal center of gravity, forward of rotor mast, in. (cm)	0.30 (0.76)
Lateral center of gravity, left of center, in. (cm)	3.81 (9.68)
Overall length, ft (m)	42.58 (12.98)
Area ratio (wing to rotor)	0.0728
Main rotor:	
Diameter, ft (m)	35 (10.67)
Blade chord (constant root to tip), in. (cm)	13.5 (34.29)
Solidity	0.0818
Blade airfoil section	Modified NACA 0012
Normal operating rotational speed, rpm	355
Blade twist (root to tip), deg	-5
Shaft incidence, forward, deg	6
Tail rotor:	
Diameter, in. (cm)	72 (182.88)
Blade chord (constant root to tip), in. (cm)	8.5 (21.59)
Solidity	0.1503
Blade airfoil section	NACA 0012
Blade twist, deg	-4.35
Wing:	
Span (nominal), ft (m)	16.83 (5.13)
Taper ratio	0.5
Area (including carry-through), ft^2 (m^2)	70 (6.5)
Aspect ratio	4.05
Airfoil	NACA 23012
Incidence (fixed), relative to fuselage reference line, deg	-0.9
Powerplants:	
Primary type	Turboshaft
Maximum shaft power (take-off) at sea level, hp (kW)	500 (373)
Military shaft power (30-min limit) at sea level, hp (kW)	450 (335.7)
Auxiliary type	Turbojet
Military thrust at 200 knots at sea level, lbf (N)	2490 (11 075.5)

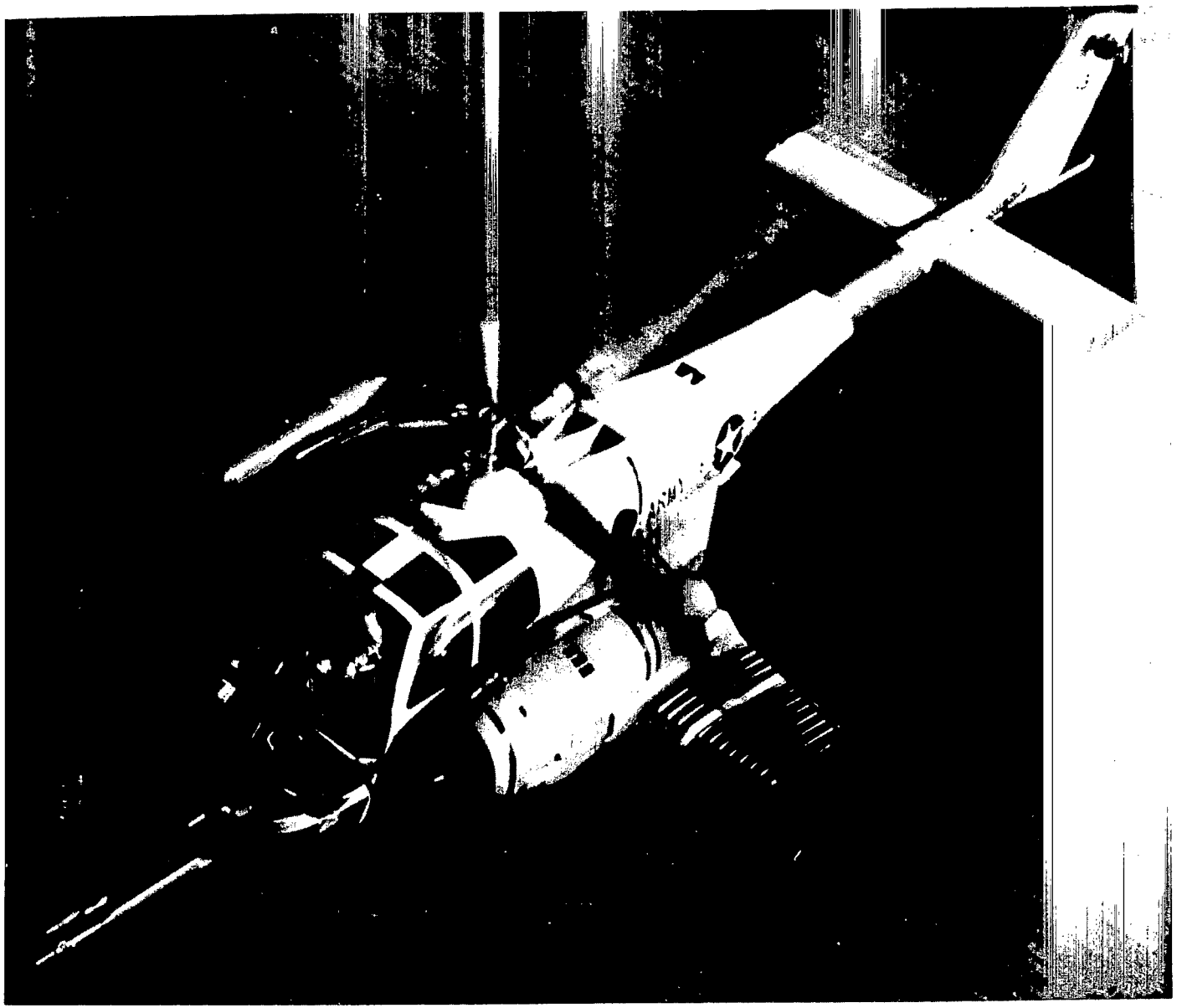

Figure 1.- Test aircraft.

L-69-5102

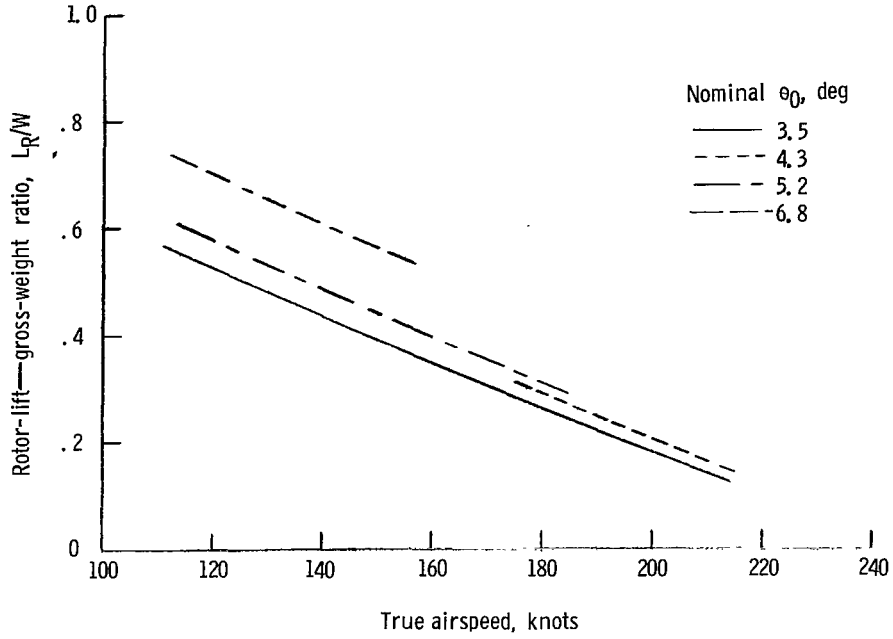

Figure 2.- Variation of level-flight rotor lift with airspeed.

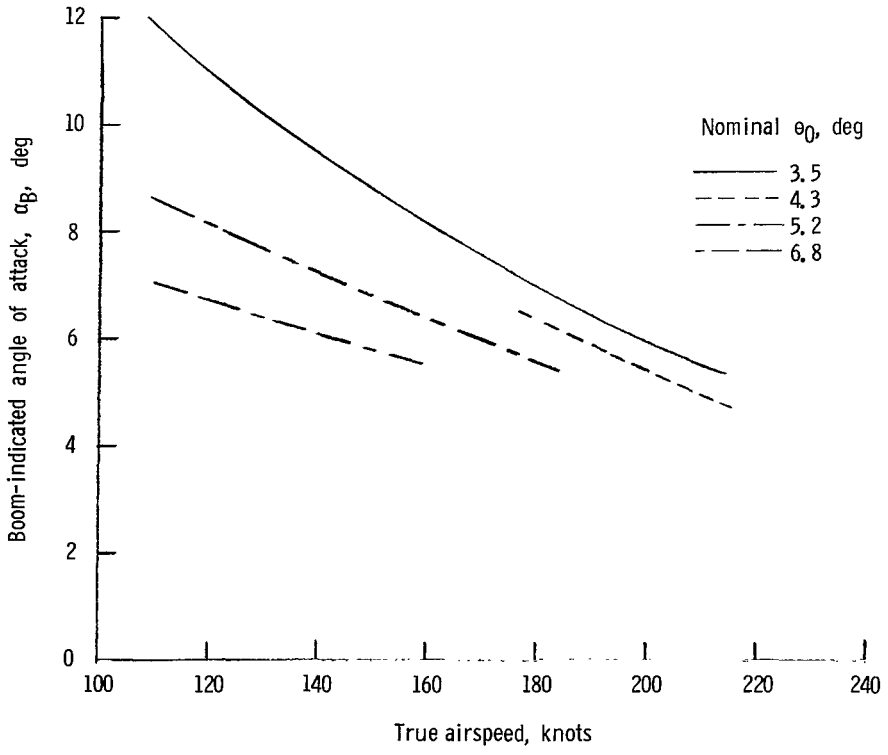

Figure 3.- Variation of level-flight angle of attack with airspeed.

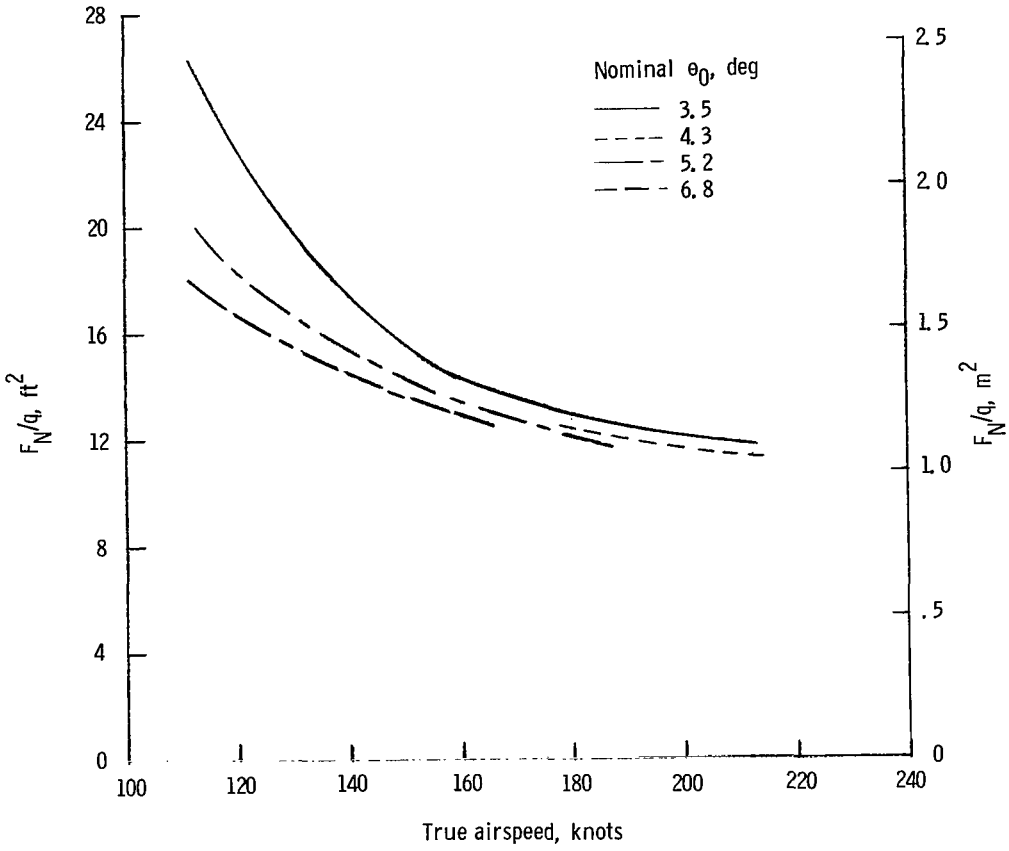

Figure 4.- Variation of level-flight auxiliary thrust (expressed as an equivalent flat-plate drag area) with airspeed.

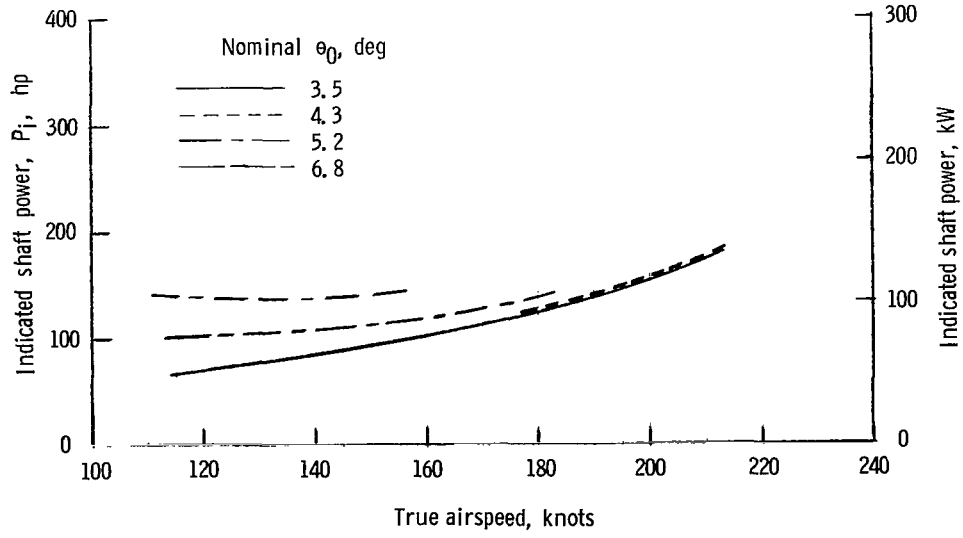

Figure 5.- Variation of level-flight main-rotor power with airspeed.

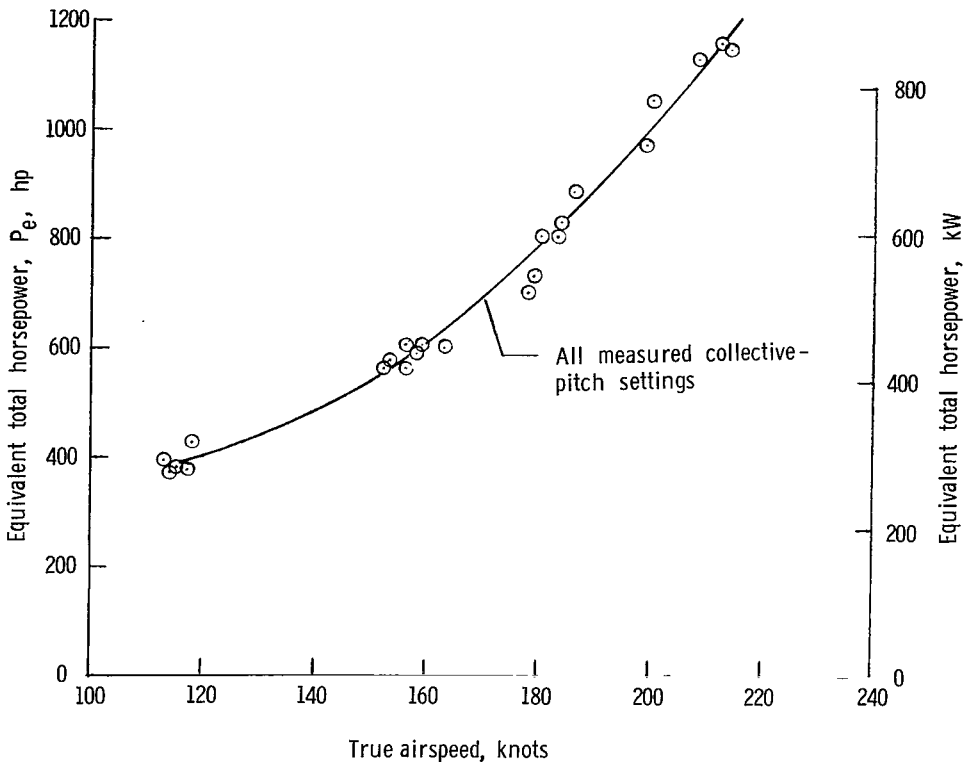

Figure 6.- Variation of level-flight equivalent total horsepower with airspeed for all measured collective-pitch settings.

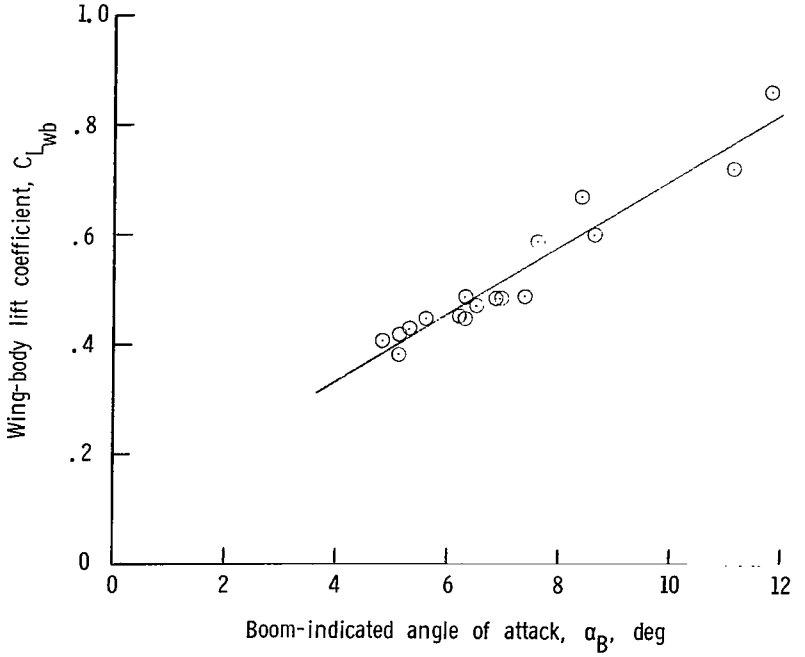

Figure 7.- Variation of wing-body lift coefficient with boom-indicated angle of attack for all test airspeeds.

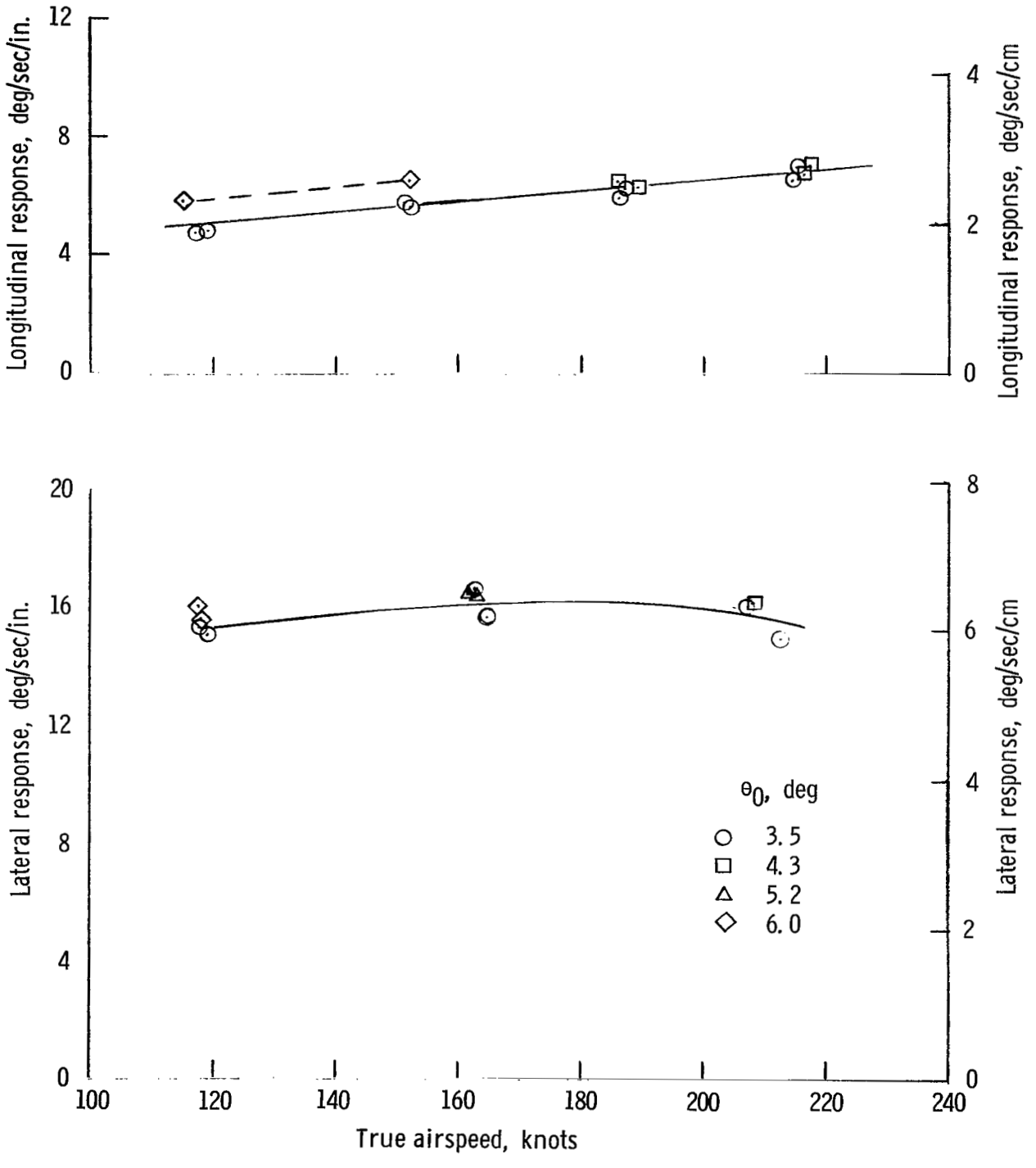

Figure 8.- Aircraft response to cyclic-stick input.

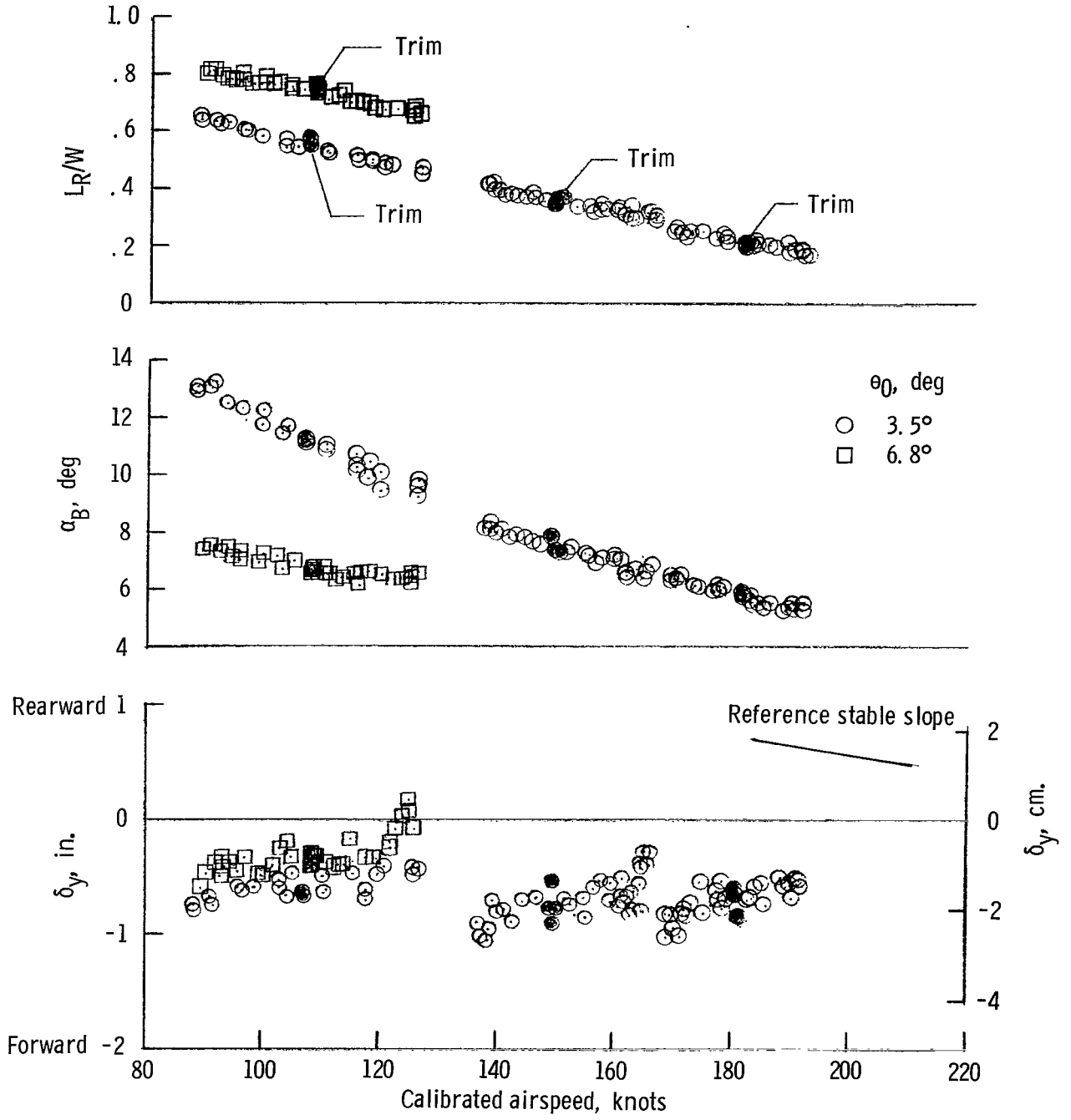

Figure 9.- Variation of rotor lift, angle of attack, and longitudinal stick position with airspeed.

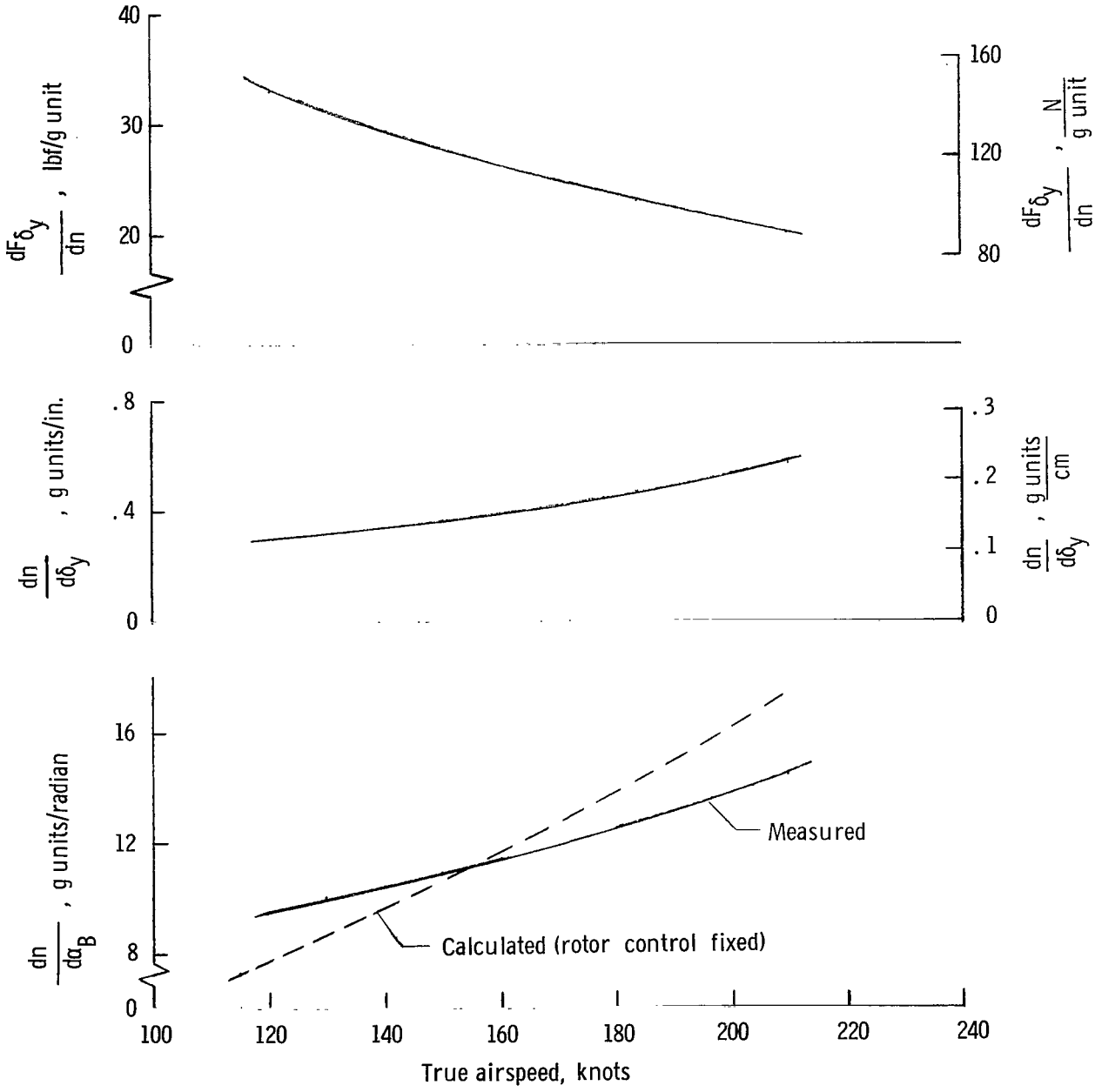

Figure 10.- Variation of airspeed maneuvering sensitivity with airspeed (windup turn).

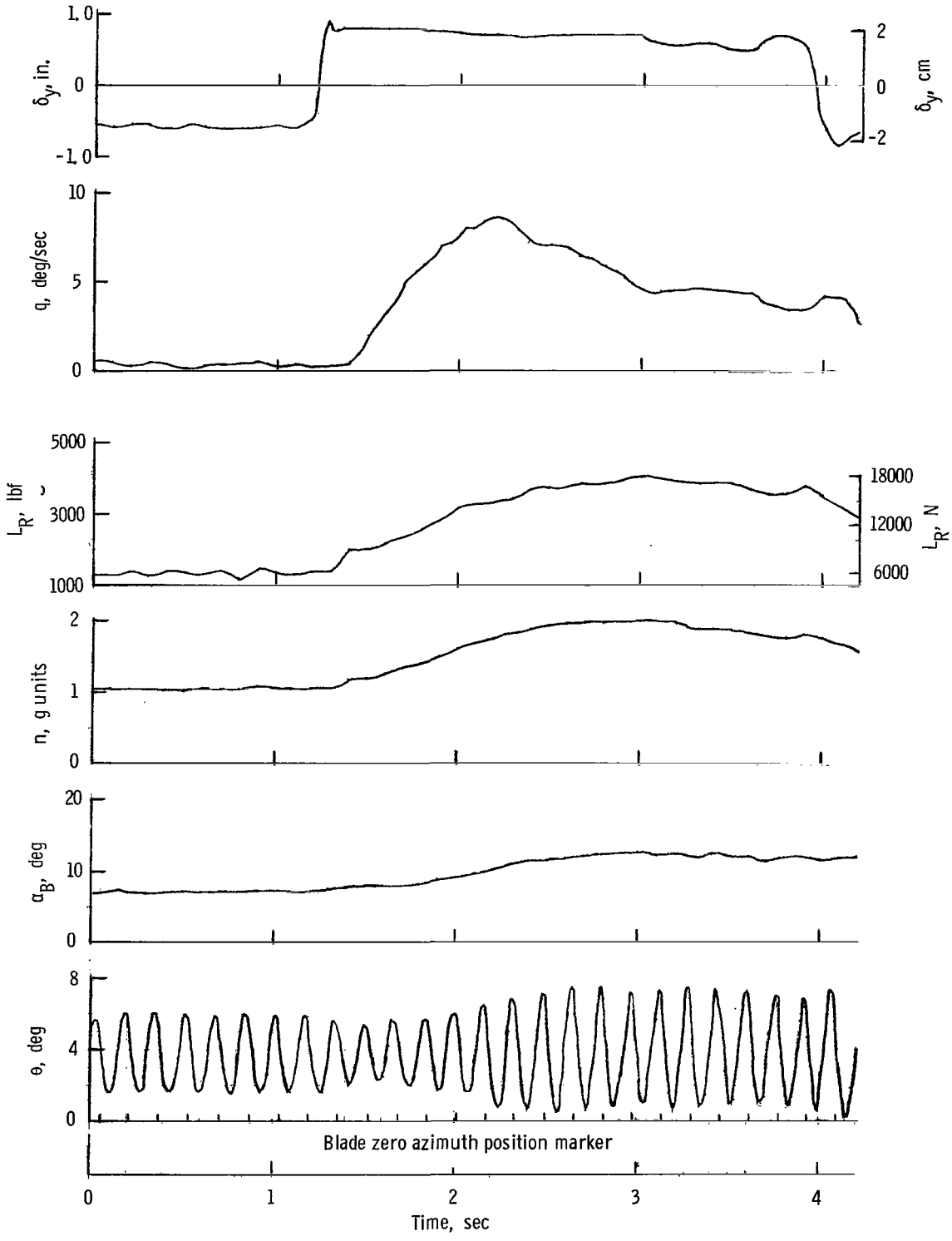

Figure 11.- Time history of longitudinal pull-and-hold maneuver. V_{CAS} = 170 knots.

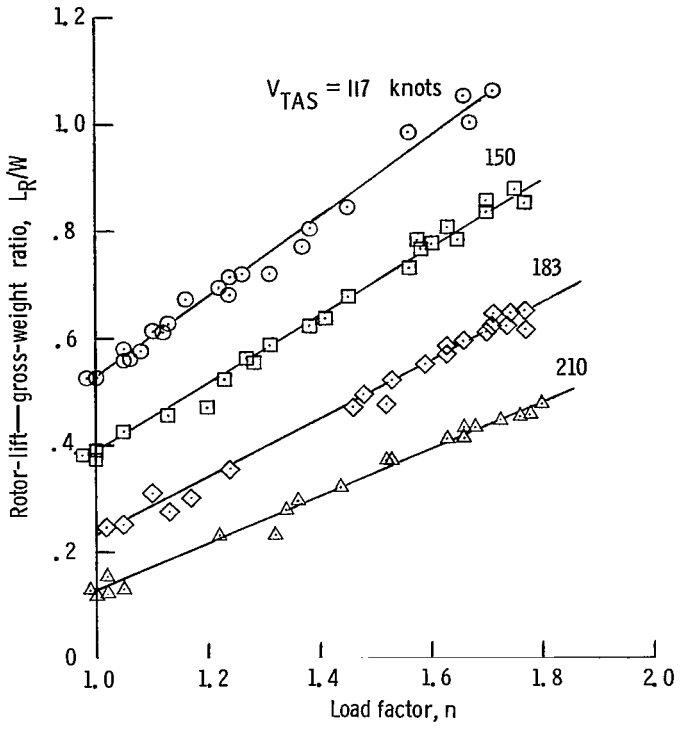

Figure 12.- Variation of rotor lift with load factor for several airspeeds. $\theta_0 = 3.5^0$; windup turn.

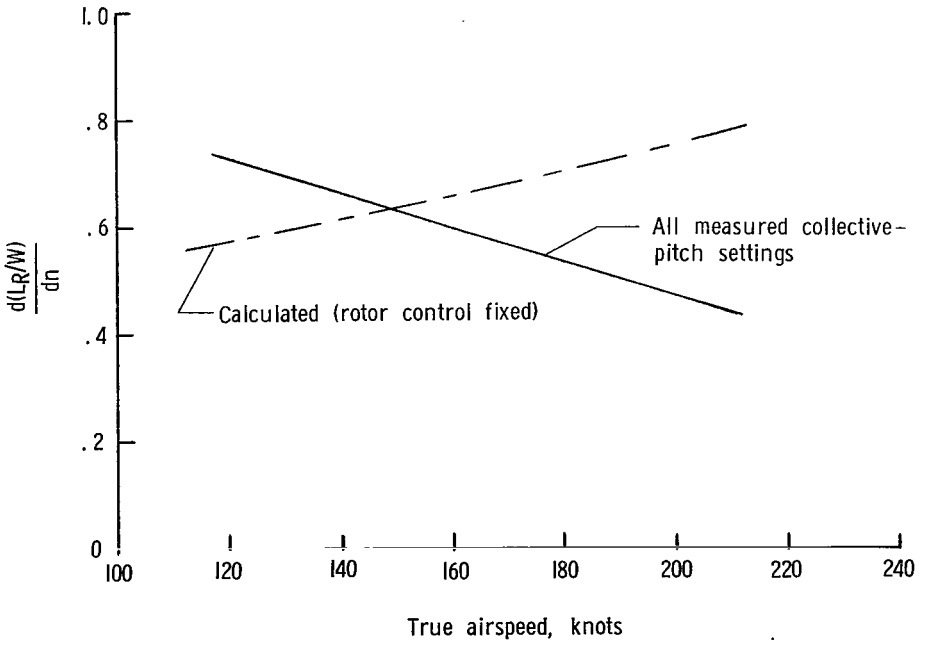

Figure 13.- Effect of airspeed on rotor-lift sensitivity in maneuvering flight.

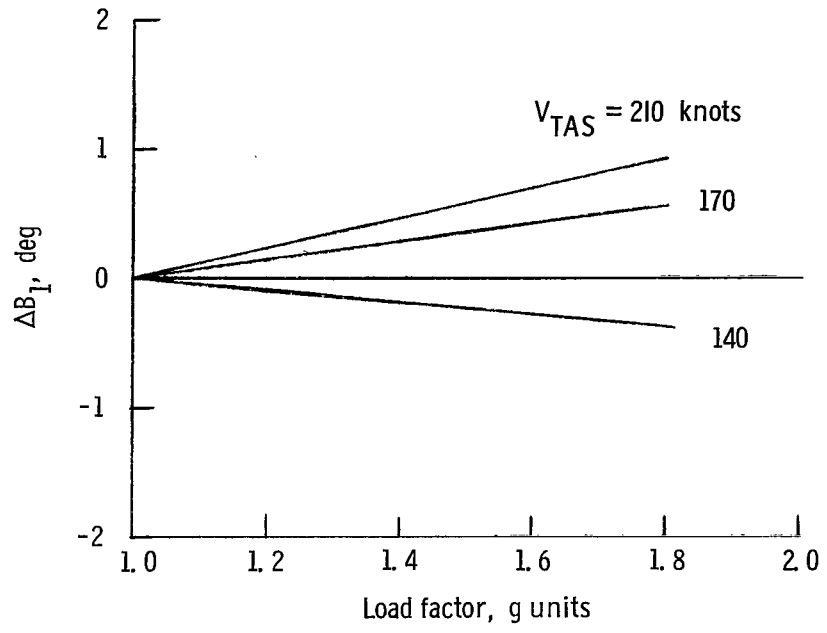

Figure 14.- Variation of longitudinal cyclic-pitch increment with load factor.

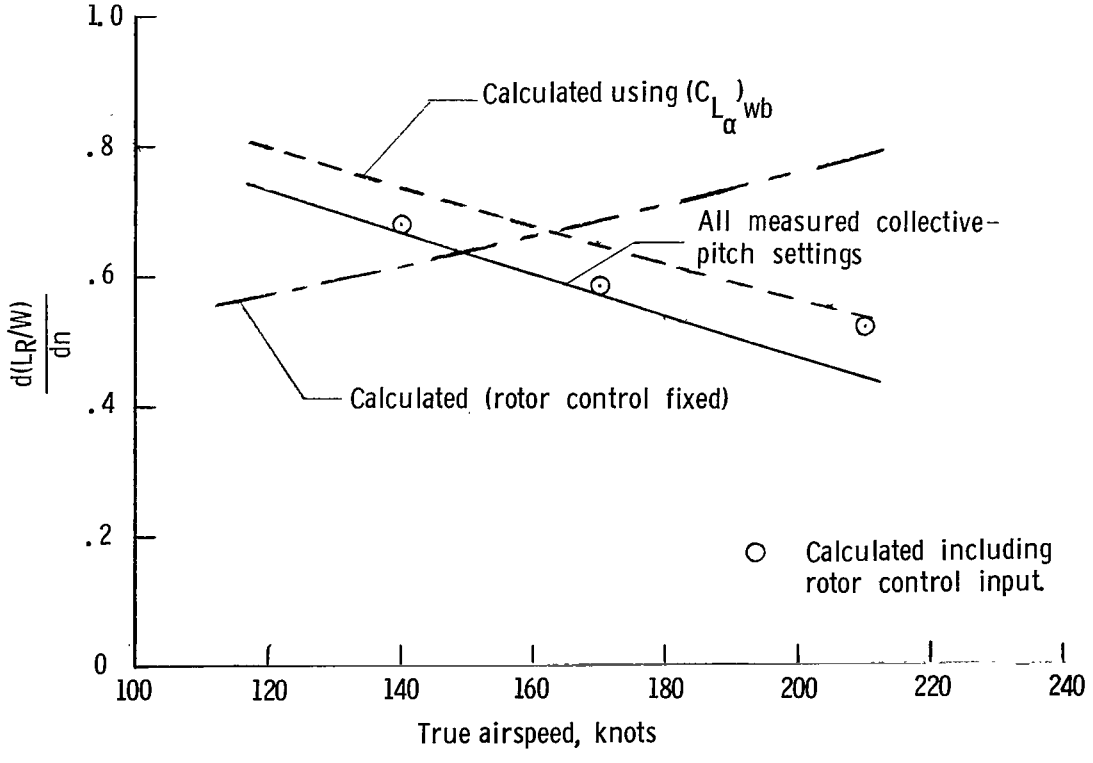

Figure 15.- Comparison of measured and calculated rotor-lift sensitivity.

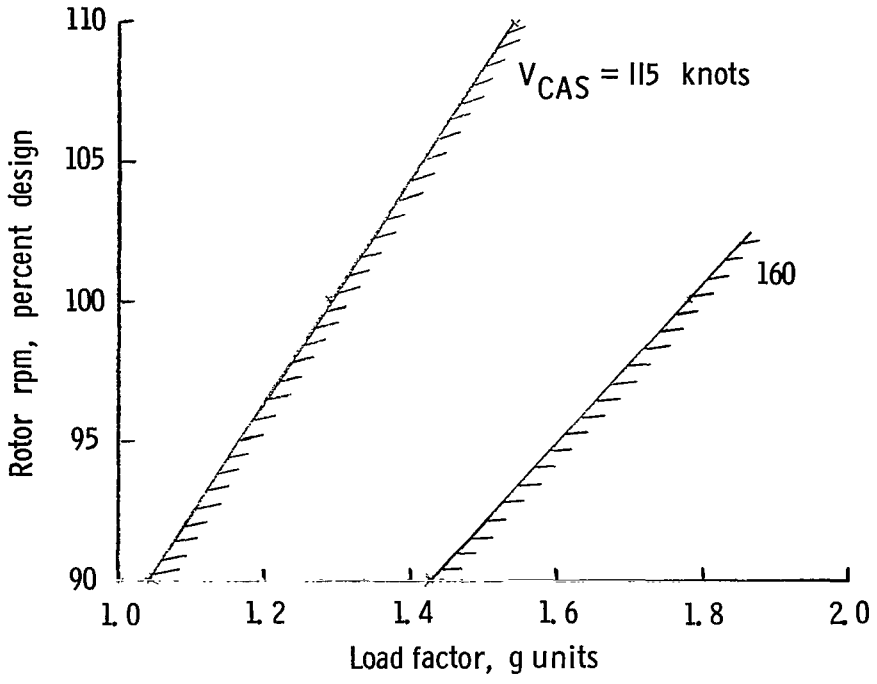

Figure 16.- Variation of power-off rotor rotational speed with load factor.

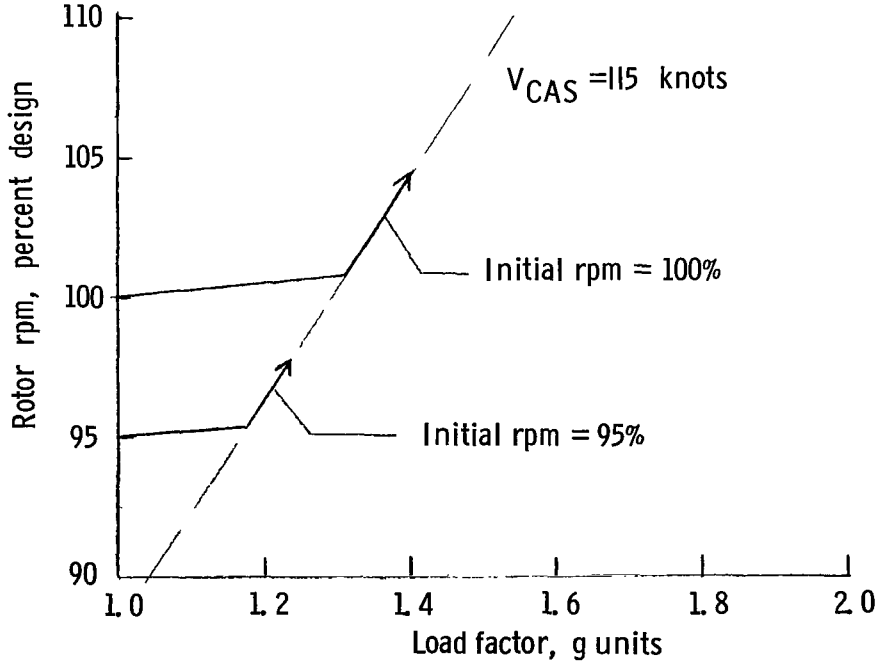

Figure 17.- Variation of power-on rotor rotational speed with load factor.

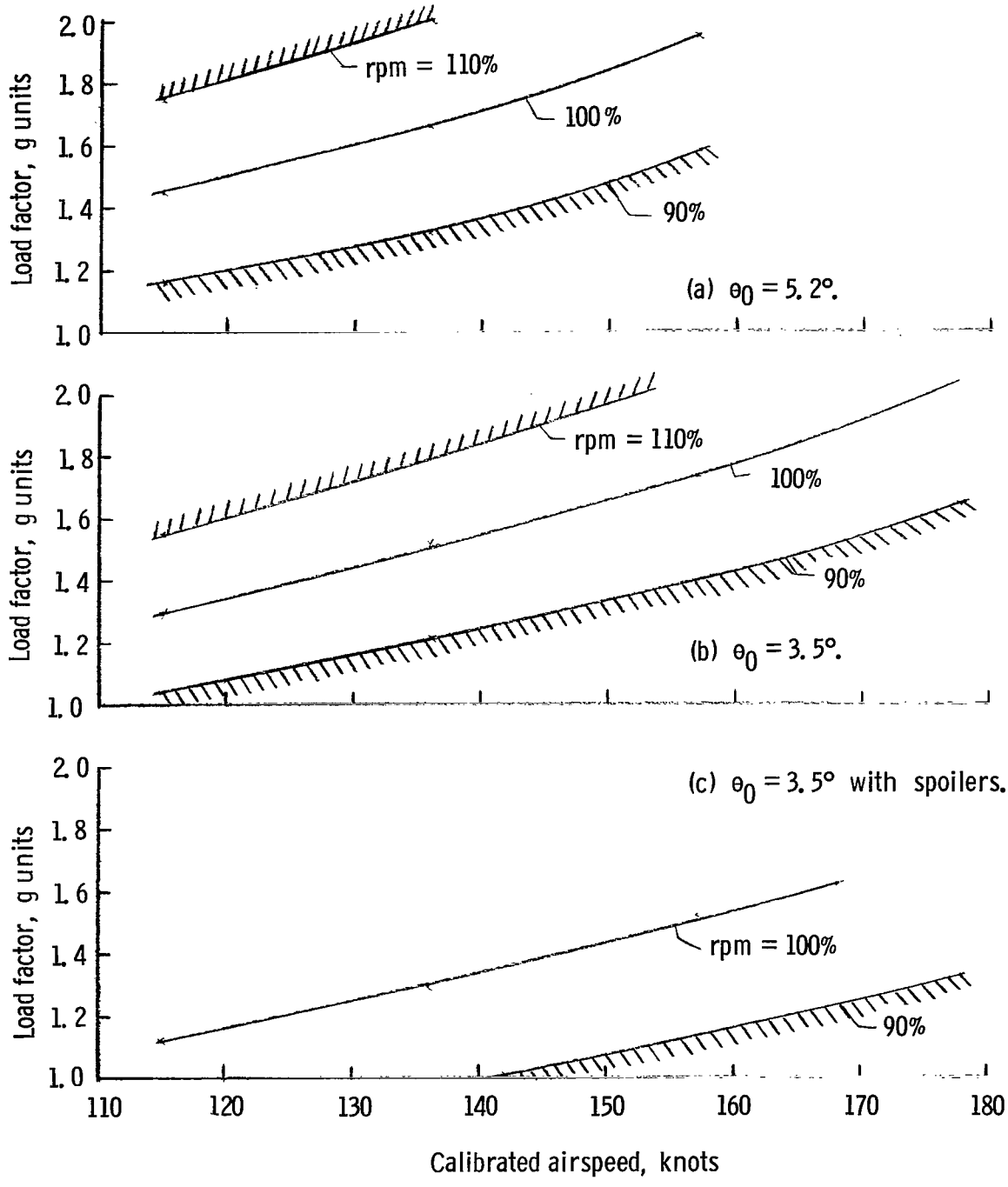

Figure 18.- Effect of aircraft configuration on rotor steady-state autorotative boundaries.

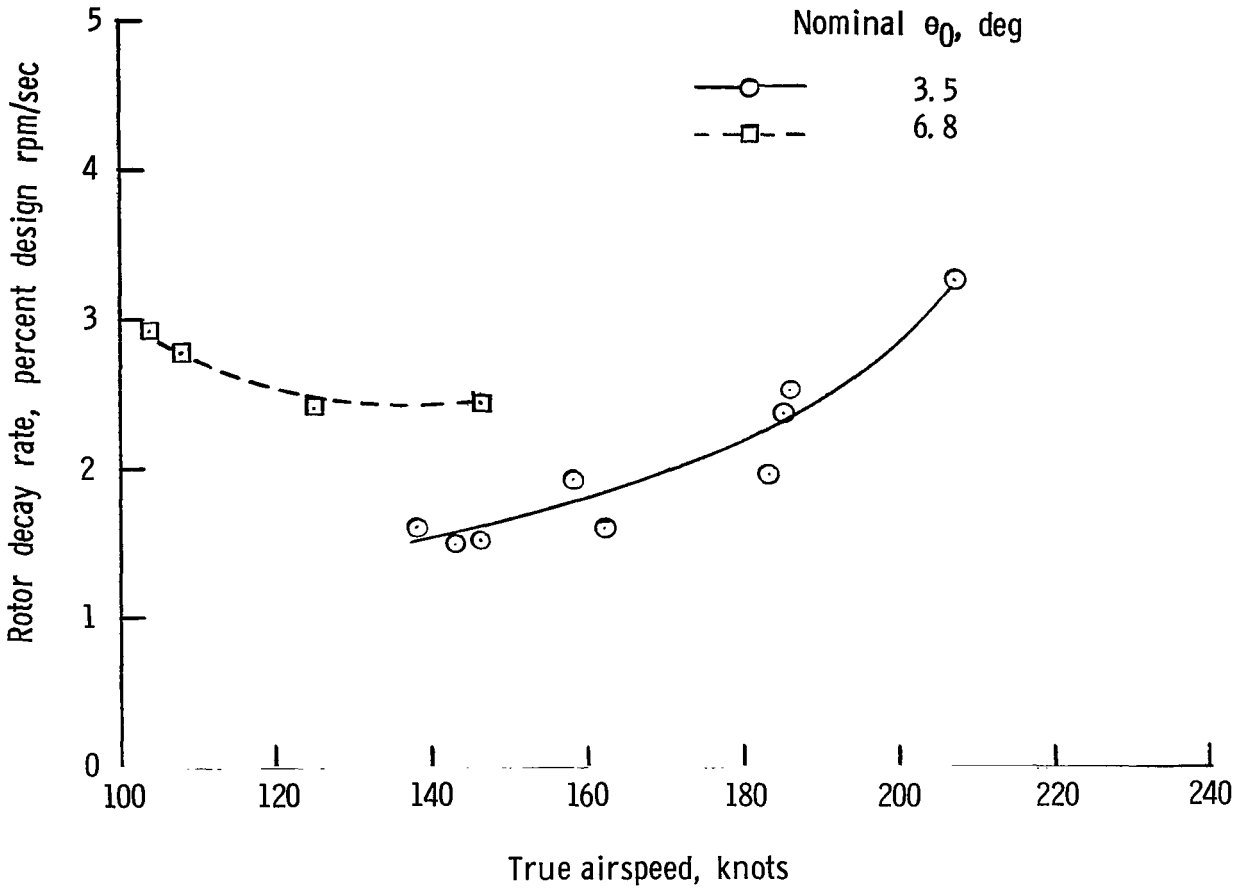

Figure 19.- Rotor rotational-speed decay rate following main-rotor throttle chop (spoilers not applied).

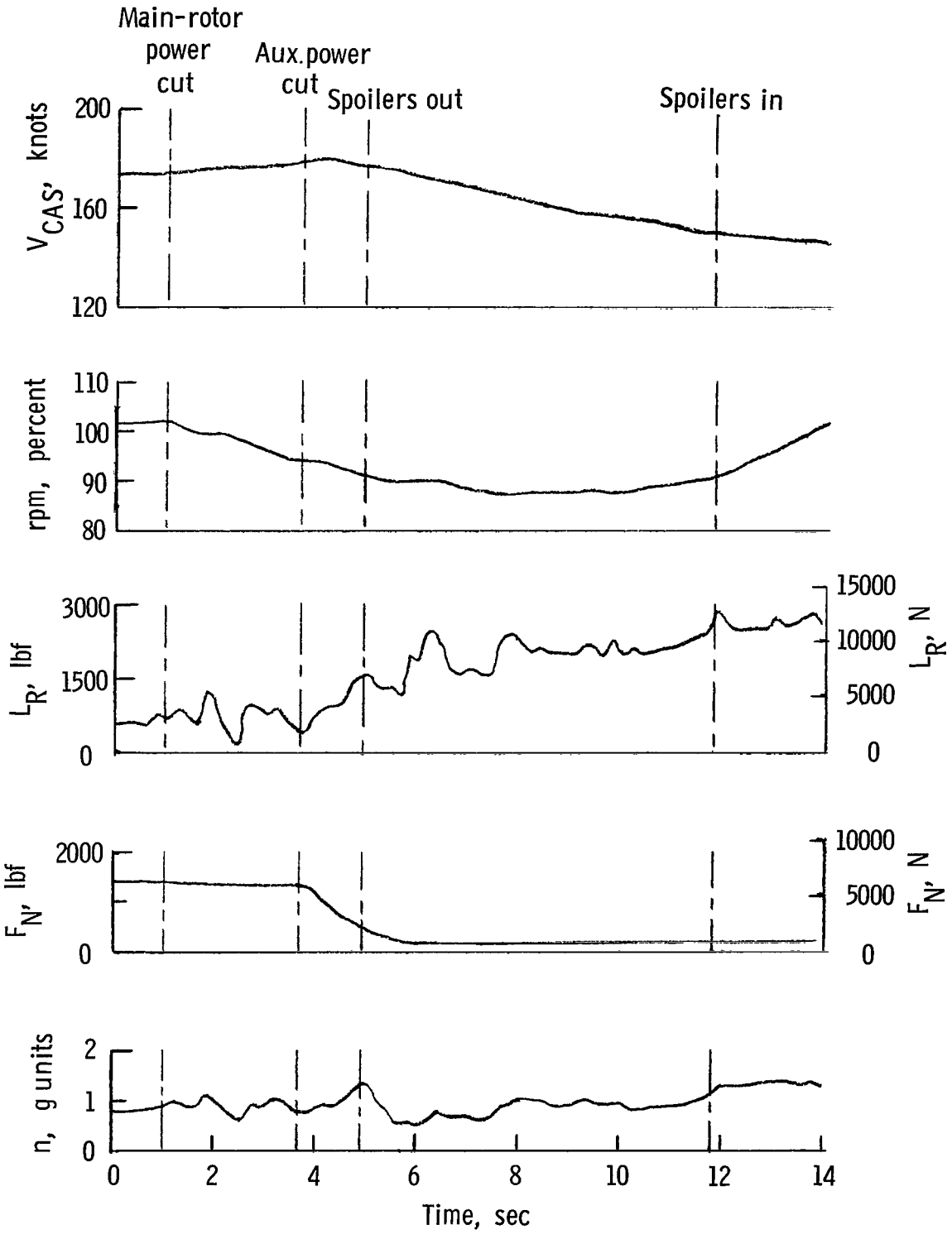

Figure 20.- Time history of autorotative entry.

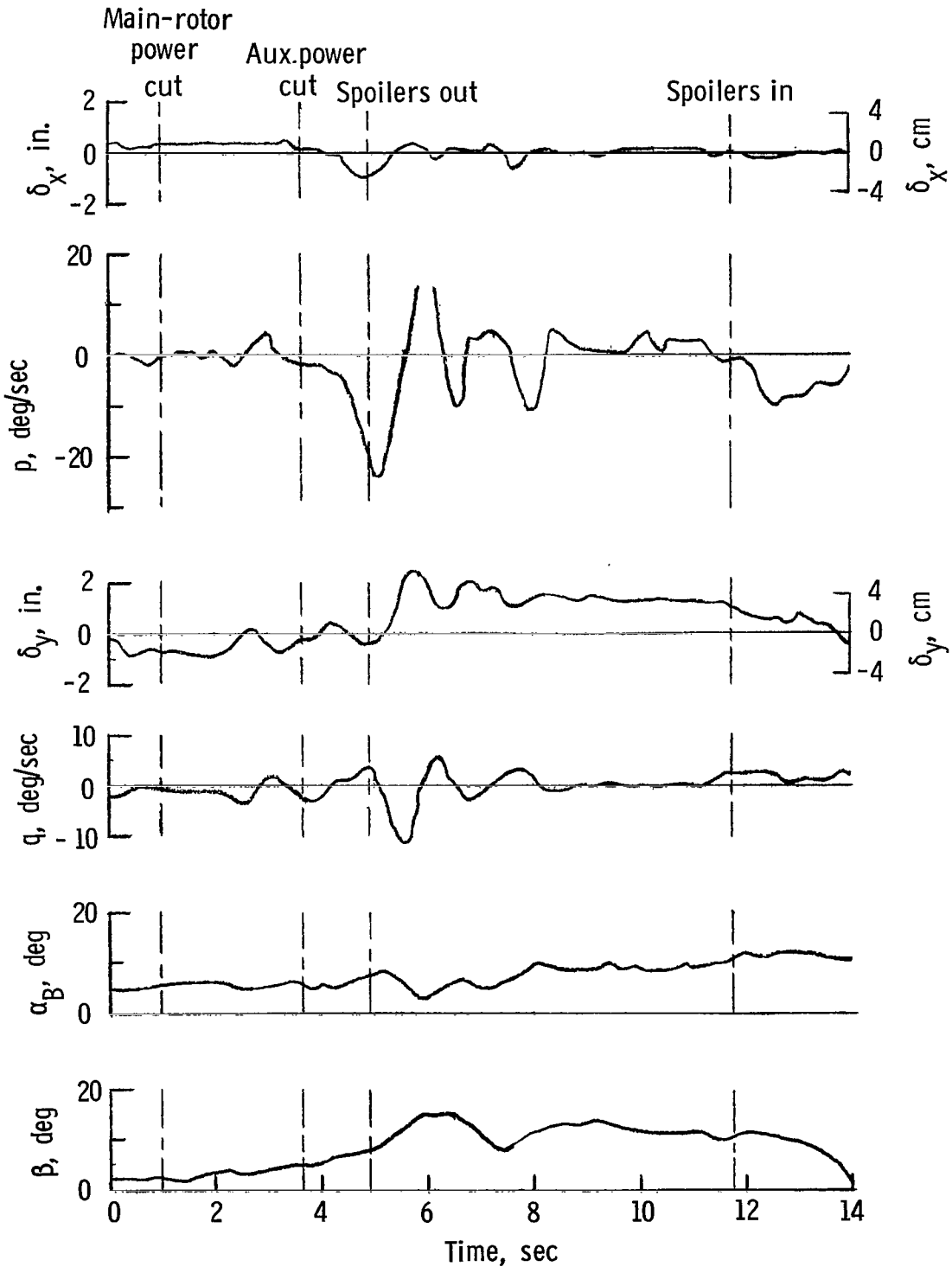

Figure 20.- Concluded.

"The aeronautical and space activities of the United States shall be conducted so as to contribute . . . to the expansion of human knowledge of phenomena in the atmosphere and space. The Administration shall provide for the widest practicable and appropriate dissemination of information concerning its activities and the results thereof."

— NATIONAL AERONAUTICS AND SPACE ACT OF 1958

NASA SCIENTIFIC AND TECHNICAL PUBLICATIONS

TECHNICAL REPORTS: Scientific and technical information considered important, complete, and a lasting contribution to existing knowledge.

TECHNICAL NOTES: Information less broad in scope but nevertheless of importance as a contribution to existing knowledge.

TECHNICAL MEMORANDUMS: Information receiving limited distribution because of preliminary data, security classification, or other reasons.

CONTRACTOR REPORTS: Scientific and technical information generated under a NASA contract or grant and considered an important contribution to existing knowledge.

TECHNICAL TRANSLATIONS: Information published in a foreign language considered to merit NASA distribution in English.

SPECIAL PUBLICATIONS: Information derived from or of value to NASA activities. Publications include conference proceedings, monographs, data compilations, handbooks, sourcebooks, and special bibliographies.

TECHNOLOGY UTILIZATION PUBLICATIONS: Information on technology used by NASA that may be of particular interest in commercial and other non-aerospace applications. Publications include Tech Briefs, Technology Utilization Reports and Notes, and Technology Surveys.

Details on the availability of these publications may be obtained from:

SCIENTIFIC AND TECHNICAL INFORMATION DIVISION

NATIONAL AERONAUTICS AND SPACE ADMINISTRATION

Washington, D.C. 20546